The Astrophysical Journal Letters, 904:L17 (6pp), 2020 December 1 https://doi.org/10.3847/2041-8213/abc6a8

Recombination-independent Determination of the Sound Horizon and the Hubble Constant from BAO

Levon Pogosian[1], Gong-Bo Zhao[2,3], and Karsten Jedamzik[4]
[1] Department of Physics, Simon Fraser University, Burnaby, BC V5A 1S6, Canada; levon@sfu.ca
[2] National Astronomy Observatories, Chinese Academy of Science, Beijing, 100101, People's Republic of China; gbzhao@nao.cas.cn
[3] University of Chinese Academy of Sciences, Beijing, 100049, People's Republic of China
[4] Laboratoire de Univers et Particules de Montpellier, UMR5299-CNRS, Universite de Montpellier, F-34095 Montpellier, France; karsten.jedamzik@umontpellier.fr
Received 2020 September 19; revised 2020 October 29; accepted 2020 October 31; published 2020 November 25

Abstract

The Hubble tension and attempts to resolve it by modifying the physics of (or at) recombination motivate finding ways to determine H_0 and the sound horizon at the epoch of baryon decoupling $r_{\rm d}$ in ways that rely neither on a recombination model nor on late-time Hubble data. In this work, we investigate what one can learn from the current and future BAO data when treating $r_{\rm d}$ and H_0 as independent free parameters. It is well known that baryon acoustic oscillations (BAOs) give exquisite constraints on the product $r_{\rm d}H_0$. We show here that imposing a moderate prior on $\Omega_{\rm m}h^2$ breaks the degeneracy between $r_{\rm d}$ and H_0. Using the latest BAO data, including the recently released the extended Baryon Oscillation Spectroscopic Survey Data Release 16, along with a $\Omega_{\rm m}h^2$ prior based on the Planck best-fit Λ cold dark matter (ΛCDM) model, we find $r_{\rm d} = 143.7 \pm 2.7$ Mpc and $H_0 = 69.6 \pm 1.8$ km s^{-1} Mpc^{-1}. BAO data prefers somewhat lower $r_{\rm d}$ and higher H_0 than those inferred from Planck data in a ΛCDM model. We find similar values when combing BAO with the Pantheon supernovae, the Dark Energy Survey Year 1 galaxy weak lensing, Planck or SPTPol cosmic microwave background lensing, and the cosmic chronometer data. We perform a forecast for the Dark Energy Spectroscopic Instrument (DESI) and find that, when aided with a moderate prior on $\Omega_{\rm m}h^2$, DESI will measure $r_{\rm d}$ and H_0 without assuming a recombination model with an accuracy surpassing the current best estimates from Planck.

Unified Astronomy Thesaurus concepts: Cosmology (343); Baryon acoustic oscillations (138); Hubble constant (758); Recombination (cosmology) (1365)

1. Introduction

The 4.2σ tension between the Hubble constant $H_0 = 73.5 \pm 1.4$ km s^{-1} Mpc^{-1} measured using Supernovae type Ia (SN) calibrated on Cepheid variable stars by the Supernovae H0 for the Equation of State (SH0ES) Collaboration (Reid et al. 2019) and the $H_0 = 67.36 \pm 0.54$ km s^{-1} Mpc^{-1} value implied by the Λ cold dark matter (ΛCDM) fit to the cosmic microwave background (CMB) anisotropy data from Planck (Aghanim et al. 2020a) prompted significant interest in new physics at the epoch of recombination (Chiang & Slosar 2018; Agrawal et al. 2019; Kreisch et al. 2019; Lin et al. 2019; Poulin et al. 2019; Sakstein & Trodden 2019; Gonzalez et al. 2020; Hart & Chluba 2020; Jedamzik & Pogosian 2020; Pandey et al. 2020; Sekiguchi & Takahashi 2020; see Di Valentino et al. 2020 for more references). This is because the value of H_0 that one gets from CMB is directly tied to the sound horizon at last scattering, which is closely related to the sound horizon at the baryon decoupling $r_{\rm d}$ that sets the characteristic scale of baryon acoustic oscillations (BAOs) in the distribution of large-scale structure. Both CMB and BAOs measure the angular size of the acoustic scale at the respective redshifts, and a smaller $r_{\rm d}$ would imply a larger H_0.

While both CMB and BAOs determine H_0 from the angular acoustic scale, there are some important differences. First, there is much more information in the CMB than just the positions of the acoustic peaks. It is generally not trivial to introduce new physics that reduces $r_{\rm d}$ without worsening the fit to other features of the temperature and polarization spectra. Second, to get any information about the H_0 from CMB spectra, it is not enough to simply know $r_{\rm d}$—one actually needs a model of the recombination, because one does not have an independent measure of the redshift of decoupling. In contrast, in the case of the BAO, one knows the redshift of the BAO feature from spectroscopy of galaxies, so there is more hope of learning something about the H_0 without relying on a recombination model.

It is well known that BAO observations constrain the product $r_{\rm d}h$, where $h \equiv H_0/(100$ km s^{-1} Mpc$^{-1})$[5]. Several strategies have been adopted to break the degeneracy between $r_{\rm d}$ and h, while avoiding using information from CMB spectra (which is based on a recombination model and measures both $r_{\rm d}$ and h exquisitely well). One option is to assume a particular recombination model, supplemented by a prior on the baryon density (Addison et al. 2013, 2018; Wang et al. 2017; Cuceu et al. 2019; D'Amico et al. 2020a; Alam et al. 2020; Ivanov et al. 2020b; Philcox et al. 2020a), which is well constrained by the big bang nucleosynthesis (BBN; Cyburt et al. 2016). This places a prior on $r_{\rm d}$, which then helps to constrain H_0. Further combining BAO and BBN with weak lensing (WL) and SN data results in tight constraints on cosmological parameters (Abbott et al. 2018a). Alternatively, one can combine BAO with measurements of the Hubble constant to infer $r_{\rm d}$ (Arendse et al. 2020; Aylor et al. 2019; Wojtak & Agnello 2019). Neither strategy is fully satisfactory as it is either model dependent or relies on observational data that is in tension. In fact, the latter method simply recasts the Hubble tension as the $r_{\rm d}$ tension. Because solutions to the Hubble tension include proposals of modified recombination, it would be preferable to have a recombination-model-independent determination of both $r_{\rm d}$ and

[5] We refer only to the measurements of the BAO peaks, not the full shape of the galaxy power spectrum. The latter also carries the imprint of the scale of the horizon at the radiation-matter equality (Philcox et al. 2020b).

H_0 using data sets that are not in tension with either SH0ES or Planck. We show that this is indeed possible.

As we show in Section 2, a prior on $\Omega_{\rm m}h^2$ helps to break the degeneracy between $r_{\rm d}$ and H_0. Treating r_d and H_0 as independent observables, we combine BAO with data capable of constraining $\Omega_{\rm m}h^2$, such as galaxy and CMB WL, in Section 3. The CMB lensing power spectra are particularly useful as they probe the largest scales of the underlying matter power spectrum, including the horizon scale at the matter-radiation equality (Baxter & Sherwin 2020). Following Zhang & Huang (2020), we also include the cosmic chronometer (OHD) data (Magana et al. 2018). In addition, we derive bounds on $r_{\rm d}$ and H_0 from BAO alone supplemented by a moderate prior on $\Omega_{\rm m}h^2$. Moderate means that it is sufficiently weak to be consistent with the Planck best-fit model, as well as viable models with modified recombination histories.

Interestingly, we find that both methods, using BAO+data and BAO+prior, give almost identical mean values for $r_{\rm d}$ and H_0 and similar 1σ uncertainties around 3 Mpc and 1.7–1.8 km s^{-1} Mpc^{-1}, respectively. We find the mean value of H_0 to be around 69.5 km s^{-1} Mpc^{-1}, lying in between the Planck and the SH0ES values. Thus, we find that, when no recombination model is assumed, the BAO data is not in significant tension with either of the two.

Furthermore, we perform a forecast for future BAO data from the Dark Energy Spectroscopic Instrument (DESI) and show that, when combined with a moderate prior on $\Omega_{\rm m}h^2$ it will constrain $r_{\rm d}$ and H_0 with precision better than Planck's, without the need for a recombination model. Future CMB experiments, such as the Simons Observatory (SO; Ade et al. 2019) and CMB-S4 (Abazajian et al. 2016), will significantly improve on the current CMB lensing reconstructions (Mirmelstein et al. 2019) and can be used along with the future galaxy WL data from Euclid[6] and Legacy Survey of Space and Time (LSST).[7] Thus, we expect excellent recombination-independent bounds on $r_{\rm d}$ and H_0 from the combination of DESI, SO/CMB-S4, and Euclid/LSST, but leave the detailed forecast to a future study.

Finally, we emphasize the importance of the $r_{\rm d}h$ parameter, which can be well measured by BAO alone along with $\Omega_{\rm m}$. As we show, current BAO data measures $r_{\rm d}h$ to a percent level accuracy. It agrees well with the ΛCDM value derived from Planck and is in tension with some alternative models. DESI will measure $r_{\rm d}h$ and $\Omega_{\rm m}$ with accuracy 4–5 times better than Planck's in a recombination-independent way, providing a powerful consistency test capable of falsifying competing models.

2. BAO Observables and the Parameter Degeneracies

The BAO scale is set by the comoving sound horizon $r_{\rm d}$ at the epoch of baryon decoupling $z_{\rm d}$, also called the "drag" epoch.[8] It is given by

$$r_{\rm d} = \int_{z_{\rm d}}^{\infty} \frac{c_S(z)dz}{H(z)}, \tag{1}$$

where the sound speed $c_S(z)$ is a known function of the baryon to photon densities ratio, and

$$H(z) = H_0\sqrt{\Omega_r(1+z)^4 + \Omega_{\rm m}(1+z)^3 + 1 - \Omega_{\rm m} - \Omega_r}\,, \tag{2}$$

where Ω_r and $\Omega_{\rm m}$ denote the present-day density fractions in relativistic and non-relativistic matter, and where we have assumed a flat ΛCDM universe, so that $\Omega_\Lambda = 1 - \Omega_{\rm m} - \Omega_r$. Often, it is useful to work in terms of the dimensionless Hubble parameter $h(z) = H(z)/(100\ {\rm km\,s^{-1}\,Mpc^{-1}})$ and the physical density parameters $\omega_i \equiv \Omega_i h^2$, where $h \equiv h(0)$. Rewriting Equation (2) as

$$h(z) = \sqrt{\omega_r(1+z)^4 + \omega_m(1+z)^3 + h^2 - \omega_m - \omega_r} \tag{3}$$

makes it apparent that, once the physical densities ω_i are provided, the value of h plays practically no role at $z > z_{\rm d} \sim 1000$ and, hence, in the integral (1). This justifies treating $r_{\rm d}$ as a parameter independent of H_0.

The BAO observables that one extracts from surveys of galaxies and other tracers of large-scale structure are of three types (Eisenstein et al. 2005): (1) the acoustic feature measured using correlations in the direction perpendicular to the line of sight,

$$\beta_\perp(z) = D_M(z)/r_{\rm d}, \tag{4}$$

where $D_M(z) = \int_0^z cdz'/H(z')$ is the comoving distance to redshift z, (2) the feature measured in the direction parallel to the line of sight,

$$\beta_\parallel(z) = H(z)r_{\rm d}, \tag{5}$$

and (3) the angle-averaged or "isotropic" measurement,

$$\beta_V(z) = D_V(z)/r_{\rm d}, \tag{6}$$

where $D_V(z) = [czD_M^2(z)/H(z)]^{1/3}$. At redshifts of relevance to galaxy surveys we can safely ignore the contribution of relativistic species in the expression for $h(z)$. Then, $\beta_\perp$ can be written as

$$\beta_\perp(z) = \int_0^z \frac{2998\ {\rm Mpc}\ dz'}{r_{\rm d}h\sqrt{\Omega_{\rm m}(1+z')^3 + 1 - \Omega_{\rm m}}} \tag{7}$$

or, equivalently, as

$$\beta_\perp(z) = \int_0^z \frac{2998\ {\rm Mpc}\ dz'}{r_{\rm d}\omega_m^{1/2}\sqrt{(1+z')^3 + h^2/\omega_m - 1}}. \tag{8}$$

From Equation (7) it is clear that having BAO measurements at multiple redshifts allows one to measure two numbers: $r_{\rm d}h$ and $\Omega_{\rm m}$. It is also evident from Equation (8) that one can break the degeneracy between $r_{\rm d}$ and h by supplementing BAO with a prior on ω_m. The same argument also applies to the other two BAO observables.

Figure 1 illustrates the above points. In the left panel we show the constraints on $r_{\rm d}h$ and $\Omega_{\rm m}$ derived from the latest BAO data (detailed in Section 3), while the right panel shows the corresponding bounds on $r_{\rm d}$ and H_0. Adding the SN data helps to constrain $\Omega_{\rm m}$, thus slightly reducing the uncertainties in the $r_{\rm d}h - \Omega_{\rm m}$ plane. As one can see from the right panel, adding a prior on $\Omega_{\rm m}h^2$ breaks the degeneracy allowing to constrain $r_{\rm d}$ and H_0 individually.

[6] http://www.euclid-ec.org

[7] http://www.lsst.org

[8] It is closely related to the sound horizon at last scattering, $r_\star \approx 1.02 r_{\rm d}$ (Anderson et al. 2014; Aubourg et al. 2015), that sets the positions of the acoustic peaks in the CMB spectra.

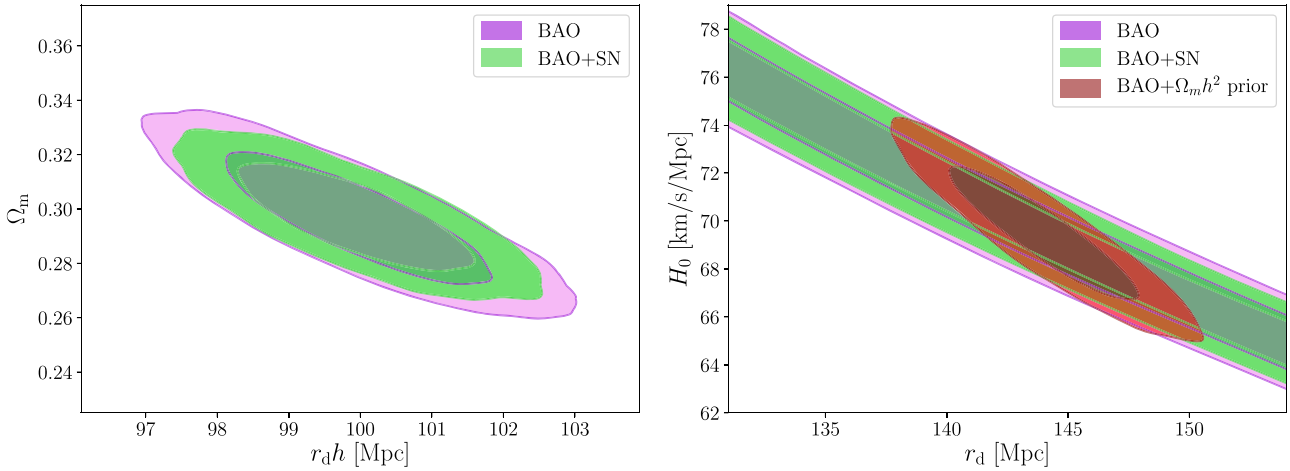

Figure 1. Constraints on $r_d h$, Ω_m, r_d, and H_0 derived from the latest combination of the BAO data, and from BAO combined with SN. The right panel shows that a prior on $\Omega_m h^2$ breaks the degeneracy between r_d and H_0.

3. Constraints from Current Data

We use a collection of BAO measurements to date, including the ones derived from the recently released Date Release 16 (DR16) of the extended Baryon Oscillation Spectroscopic Survey (eBOSS; Alam et al. 2020). Being a multi-tracer galaxy survey, eBOSS provides BAO and redshift space distortion (RSD) measurements at multiple redshifts from the samples of luminous red galaxies (LRGs), emission line galaxies (ELGs), clustering quasars (QSOs), and the Lyα forest. In this work, we use the BAO measurement from the full-shape auto- and cross-power spectrum of the eBOSS LRGs and ELGs (Zhao et al. 2020; Wang et al. 2020), the BAO measurement from the QSO sample (Hou et al. 2020), and from the Lyα forest sample (du Mas des Bourboux et al. 2020). As all of these measurements are at $z > 0.6$, we combine them with low-z measurements, including the BAO measurement by 6dF (Beutler et al. 2011), Sloan Digital Sky Survey Data Release 7 (SDSS DR7) main Galaxy sample (MGS; Ross et al. 2015) as a complement.

As explained in Section 2, BAOs on their own can constrain Ω_m and the product $r_d h$. To constrain r_d and H_0 individually, one can either supplement BAOs with data that provides a prior on $\Omega_m h^2$, or data that constrains H_0, or the combination of the two. Restricting to data sets that do not rely on modeling the recombination physics, the first option includes the galaxy and the CMB WL data. To that aim, we consider the Dark Energy Survey Year 1 galaxy clustering and WL data (DES; Abbott et al. 2018b), and the CMB lensing power spectra from Planck 2018 (PL; Aghanim et al. 2020b) and SPTpol (SL; Wu et al. 2019; Bianchini et al. 2020). Both types of measurements are practically insensitive to the scale of baryon decoupling and primarily probe the cumulative clustering of matter. While, in principle, a different redshift of decoupling would change the time at which baryons begin to cluster, this is a very minor effect on the net growth of cosmic structures dominated by dark matter. For the second option, to avoid data contributing to the Hubble tension, we use the cosmic chronometer data (OHD) from Moresco et al. (2016) and Ratsimbazafy et al. (2017). The latter contain determinations of $H(z)$ at 31 redshifts in the $0.1 \lesssim z \lesssim 2$ range and, because Ω_m and H_0 are the only parameters in our flat Friedmann–Robertson–Walker (FRW) model, provides a handle on the value of H_0 when combined with the BAO.

We use `CosmoMC` (Lewis & Bridle 2002) modified to work with r_d as an independent parameter. The cosmological parameters that we vary are r_d, H_0 and either Ω_m or $\Omega_m h^2$. When using the DES and CMB lensing data, we additionally vary the amplitude of the primordial fluctuations spectrum A_s and the spectral index n_s. As was shown in Ade et al. (2016), CMB lensing constrains the combination of $A_s(\Omega_m^{0.6} h)^{2.3}$, where A_s is the primordial fluctuations spectrum amplitude. Further combining it with galaxy lensing helps to constrain A_s and deliver a prior on $\Omega_m h^2$. We also use the Pantheon SN sample (Scolnic et al. 2018) which does not help in breaking the r_d-H_0 degeneracy but still helps a little bit by providing an independent constraint on Ω_m. We find that the combination of the SN, DES, and PL data gives $\Omega_m h^2 = 0.140 \pm 0.011$ at 68% confidence level (CL). This constraint is an order of magnitude weaker than that derived from the Planck CMB anisotropies, but future WL data will do significantly better.

Figure 2 shows the effect of combing BAOs with WL data, namely BAO+SN+DES, BAO+SN+DES+PL, and BAO+SN +DES+SL, and with the OHD data, as well as their combination. The comprehensive list of parameter constraints from various data combinations is given in Table 1. Clearly, the OHD data dominates the constraints when included. We also note that BAO+SN+SL prefers a somewhat higher H_0 and smaller r_d, while still being quite consistent with BAO+SN+PL. The mean values obtained from BAO+SN+OHD and BAO+SN+DES+PL (+SL) also show a good consistency with each other, although the uncertainties in the latter are large. Combining all the data together, we find $H_0 = 69.3/69.6 \pm 1.7$ and $r_d = 144.4/143.6^{+2.8}_{-3.4/3.3}$ from BAO+SN+DES+PL/SL+OHD.

In addition to analyzing the above-mentioned combinations of data sets, we separately consider the BAO data supplemented by several externally imposed Gaussian priors on $\Omega_m h^2$. Figure 3 shows the posterior distributions of the relevant parameters derived using two choices of priors: one based on the Planck best-fit ΛCDM (Aghanim et al. 2020a) and the other on an alternative recombination model that also gives an acceptable fit to the CMB (Jedamzik & Pogosian 2020). The plot shows that the results are not very sensitive to the choice of the prior. Table 1 shows results with two different fixed values of $\Omega_m h^2$, and priors of doubled width, all giving comparable outcomes. This indicates that the uncertainties are dominated by those in the current BAO data. As we will see in the next

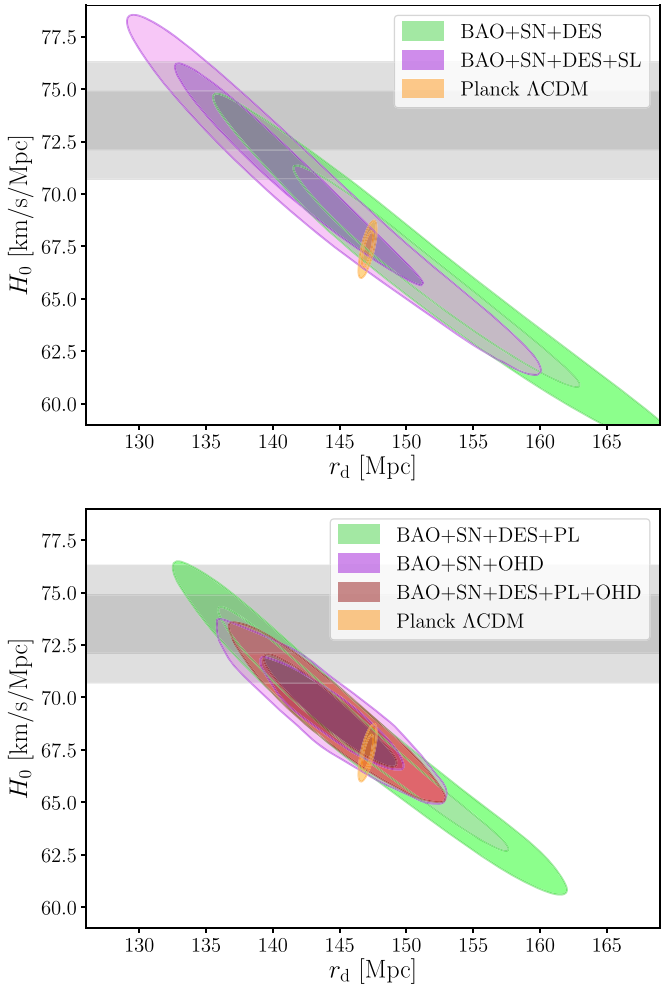

Figure 2. Constraints on r_d and H_0 derived from the BAO data combined with Pantheon SN, DES galaxy WL, CMB WL from Planck and SPTPol, and the OHD data. The gray bands show the 68% and 95% CL determination of H_0 by SH0ES. The ΛCDM based bound from Planck CMB anisotropy spectra is shown for reference.

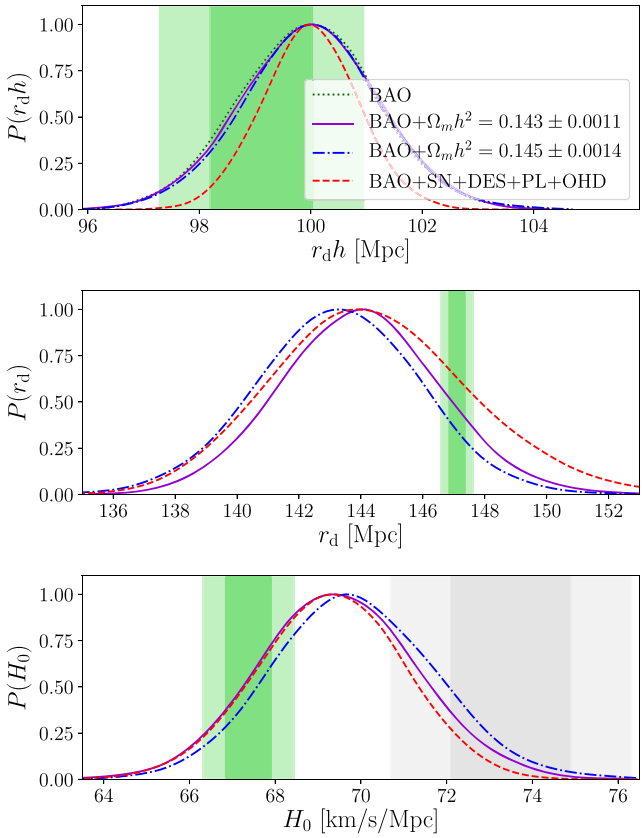

Figure 3. Constraints on $r_d h$, r_d, and H_0 from BAO and different priors on $\Omega_m h^2$. The constraint from a combination of current recombination-independent data is shown as well. The green vertical bands correspond to the Planck best-fit ΛCDM. The gray bands show the H_0 measurement by SH0ES.

section, the strength of the $\Omega_m h^2$ prior will play a more important role for future BAO data from DESI.

Imposing a prior on $\Omega_m h^2$ is, to some extent, a matter of choice. While $\Omega_m h^2$ has the well-defined physical meaning of the present-day matter density, imposing a prior on another combinations of Ω_m and h would also do the job. In fact, a study dedicated to the consistency test between CMB and BAO could benefit from combining the latter with a prior on $\Omega_m h^3$, which is the combination best constrained by CMB in a flat FRW cosmology (Percival et al. 2002). We leave exploring this possibility to a separate investigation.

It is worth noting that the CMB-derived best-fit value of $\Omega_m h^2$ is quite consistent between a number of models with modified recombination histories.[9] This further justifies applying a prior on $\Omega_m h^2$ when attempting to gain recombination-model-independent information from BAO. It also provides a consistency test with the results obtained by combining BAO with the WL and the OHD data.

[9] It is notably larger in early dark energy (EDE) models, which puts them in tension with the galaxy WL data (D'Amico et al. 2020b; Hill et al. 2020; Ivanov et al. 2020a; Ye & Piao 2020; see also Murgia et al. 2020; Smith et al. 2020 for an alternative perspective).

For comparison, in Figure 3, we also show the constraints from the BAO+SN+DES+PL/SL+OHD, which are largely the same as those derived using the $\Omega_m h^2$ prior. Both methods give $r_d \approx 144 \pm 3$ Mpc and $H_0 \approx 69.5 \pm 1.8$ km s^{-1} Mpc^{-1}. The latter number is in between and within the 1–2σ range of the Planck and SH0ES values, shown with vertical bands.

As the top panel in Figure 3 shows, BAO alone can constrain the product $r_d h$ to a percent level accuracy, yielding a value that is in a perfect agreement with Planck's ΛCDM. We note that $r_d h$, if measured with sufficient accuracy, can be used to discriminate between models. As we will show in the forecast section, DESI alone will determine $r_d h$ and Ω_m with accuracy several times better than Planck's providing a powerful consistency test without any assumptions about recombination physics.

4. Forecast for DESI

In this section, we perform a Fisher forecast for r_d and H_0, as well as $r_d h$ and Ω_m, using the specifications of DESI (Aghamousa et al. 2016), an upcoming stage-IV galaxy survey. We assume that DESI will survey 14,000 deg^2 of the sky, using the bright galaxies (BGs; $z \lesssim 0.45$), LRGs ($0.65 \lesssim z \lesssim 1.15$), and ELGs ($0.65 \lesssim z \lesssim 1.65$), and that we are able to extract the tomographic information on the past light cone at a redshift resolution of $\Delta z \lesssim 0.1$. In this forecast, we used the full-shape anisotropic galaxy power spectrum as observable, and marginalize over the RSD, bias and Fingers-of-God parameters.

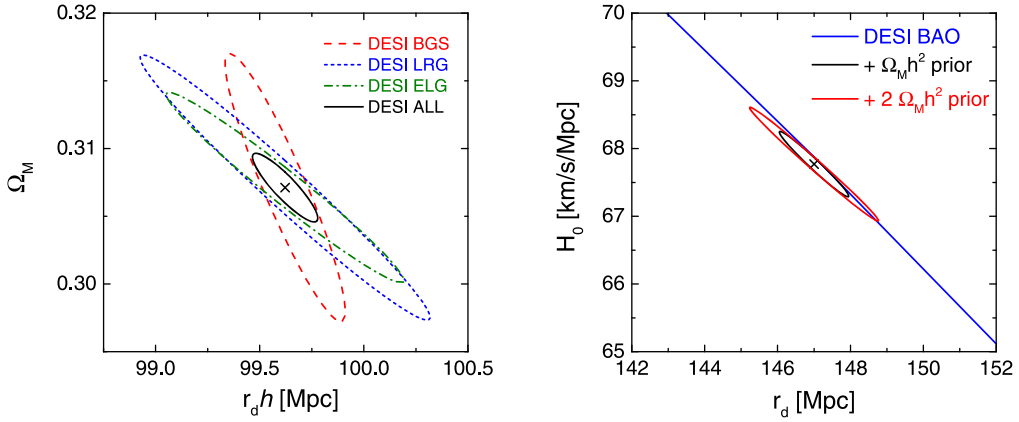

Figure 4. Forecasted constraints on $\{r_d h, \Omega_m\}$ (left panel) and $\{r_d, H_0\}$ (right panel) using specification of the DESI survey. The contours represent the 68% CL constraint, and the crosses mark the fiducial model. In the right panel, different priors on $\Omega_m h^2$ are applied, where "$\Omega_m h^2$ prior" means the Gaussian prior on $\Omega_m h^2$ from the Planck 2018 observations, namely, $\sigma_{\Omega_m h^2} = 0.0011$, and "$2\Omega_m h^2$ prior" means the 2σ Planck prior.

Table 1
Mean Parameter Values and 68% CL Uncertainties Derived from the Considered Combinations of Data Sets

	$r_d h$ (Mpc)	Ω_m	r_d (Mpc)	H_0 (km s^{-1} Mpc^{-1})
BAO	99.95 ± 1.2	$0.297^{+0.014}_{-0.016}$	…	…
BAO+SN	99.9 ± 1.0	0.297 ± 0.013	…	…
BAO+SN+DES	100.1 ± 1.0	$0.294^{+0.011}_{-0.012}$	$152.3^{+6.2}_{-7.6}$	65.9 ± 3.4
BAO+SN+PL	100.0 ± 1.0	0.295 ± 0.012	$151.3^{+7.8}_{-4.2}$	$66.2^{+1.8}_{-3.6}$
BAO+SN+SL	99.9 ± 1.1	0.297 ± 0.013	$145.5^{+6.7}_{-9.1}$	68.8 ± 3.6
BAO+SN+OHD	99.9 ± 1.0	0.298 ± 0.013	144.4 ± 3.4	69.2 ± 1.7
BAO+SN+DES+PL	99.9 ± 1.0	0.297 ± 0.012	$145.9^{+5.0}_{-8.3}$	$68.6^{+4.1}_{-3.2}$
BAO+SN+DES+SL	100.2 ± 1.0	$0.292^{+0.011}_{-0.014}$	$142.1^{+4.0}_{-7.3}$	$70.7^{+4.0}_{-2.7}$
BAO+SN+DES+PL+OHD	99.99 ± 0.84	0.2961 ± 0.0083	$144.4^{+2.8}_{-3.4}$	69.3 ± 1.7
BAO+SN+DES+SL+OHD	99.96 ± 0.85	0.2960 ± 0.0083	$143.6^{+2.8}_{-3.3}$	69.6 ± 1.7
BAO+fixed $\Omega_m h^2 = 0.143$	100.1 ± 1.2	$0.294^{+0.014}_{-0.016}$	143.7 ± 2.5	69.7 ± 1.8
BAO+prior $\Omega_m h^2 = 0.143 \pm 0.0011$	100.0 ± 1.2	$0.294^{+0.014}_{-0.016}$	143.8 ± 2.6	69.6 ± 1.9
BAO+prior $\Omega_m h^2 = 0.143 \pm 0.0022$	99.99 ± 1.2	$0.294^{+0.014}_{-0.016}$	143.7 ± 2.7	69.6 ± 1.8
BAO+fixed $\Omega_m h^2 = 0.145$	99.95 ± 1.2	0.295 ± 0.016	142.9 ± 2.5	70.0 ± 1.8
BAO+prior $\Omega_m h^2 = 0.145 \pm 0.0014$	100.0 ± 1.2	$0.294^{+0.015}_{-0.017}$	142.9 ± 2.6	70.0 ± 1.9
BAO+prior $\Omega_m h^2 = 0.145 \pm 0.0028$	100.0 ± 1.2	$0.294^{+0.014}_{-0.016}$	142.7 ± 2.8	70.1 ± 1.9

The forecast results are shown in Figure 4 and Table 2. We find that DESI alone will be able to measure $r_d h$ in a recombination-independent way with an accuracy of ∼0.1%, almost an order of magnitude better than Planck, providing an important consistency check. DESI will also constrain Ω_m with a five-fold improvement in accuracy over Planck.

With the help of a Gaussian prior on $\Omega_m h^2$, based on the present estimate from Planck (Aghanim et al. 2020a), DESI will measure r_d and H_0 with 1σ uncertainties of ∼0.6 Mpc and ∼0.3 km s^{-1} Mpc^{-1}, respectively. Unlike the case with the current BAO data, which we saw not to be particularly sensitive to the width of the $\Omega_m h^2$ priors, the results from DESI will be directly dependent on it. As Figure 4 and Table 2 show, doubling the width of the prior doubles the uncertainties in r_d and H_0. Even then, DESI would yield results with accuracy that is comparable to Planck's.

The sensitivity of DESI to the prior on $\Omega_m h^2$ prompts one to seek alternative ways to constrain it to a similar accuracy. The additional information could come from the CMB WL spectra from SO and CMB-S4, which will improve considerably on Planck lensing (Mirmelstein et al. 2019), as well as galaxy lensing from Euclid and LSST.

Table 2
Forecast for $\{r_d h, \Omega_m\}$ and $\{r_d, H_0\}$ Using Different DESI Tracers with Planck Priors on $\Omega_m h^2$

Parameter	BG	LRG	ELG	ALL
$\sigma(r_d h)$	0.192	0.464	0.380	0.105
$\sigma(\Omega_m)$	0.0066	0.0065	0.0047	0.0017
	$+\sigma(\omega_m)$	$+2\sigma(\omega_m)$		
$\sigma(r_d)$	0.636	1.179		
$\sigma(H_0)$	0.323	0.560		

5. Summary

We have shown that there is a wealth of information that one can extract from the BAO data without using information that depends on a particular recombination model. In particular, one can measure r_d and H_0 from the BAO by supplementing it with a prior on $\Omega_m h^2$. This can be done by combining BAO with the lensing information from either the CMB or the galaxies, or imposing a moderate Gaussian prior based on a consensus determination of $\Omega_m h^2$ from CMB. We find that the combination of BAO, SN, OHD, DES,

and PL (or SL) give competitive determinations of both parameters, with $r_{\rm d} \approx 144.4^{+2.8}_{-3.4}$ ($143.6^{+2.8}_{-3.3}$) Mpc and $H_0 \approx 69.3 \pm 1.7$ (69.6 ± 1.7) km s^{-1} Mpc^{-1}, showing an excellent consistency with $r_{\rm d} \approx 143.8 \pm 2.6$ Mpc and $H_0 \approx 69.6 \pm 1.9$ km s^{-1} Mpc^{-1} obtained using the BAO+prior method. They are also consistent at 1σ level with the Planck best-fit ΛCDM values of $r_{\rm d} = 147.10 \pm 0.27$ Mpc and $H_0 = 67.37 \pm 0.54$ km s^{-1} Mpc^{-1}.

We found that current BAO data provides a competitive constraint on the product $r_{\rm d}h$, showing a good agreement with the best-fit ΛCDM value from Planck. We have also performed a forecast for DESI, finding that it will constrain $r_{\rm d}h$ and $\Omega_{\rm m}$ with an order of magnitude better accuracy that will allow for a powerful consistency check against parameters determined from CMB.

Future CMB experiments, like the SO (Ade et al. 2019) and CMB-S4 (Abazajian et al. 2016) will significantly improve on the current CMB lensing reconstructions (Mirmelstein et al. 2019), while Euclid and LSST will provide much better galaxy lensing data. It will be interesting to perform a detailed forecast for DESI+SO/S4+Euclid/LSST using $r_{\rm d}$ as an independent variable. We leave this to a future study.

It is evident that a recombination-model-independent determination of $r_{\rm d}$ and H_0 prefers somewhat larger H_0 and smaller $r_{\rm d}$ than Planck data under the assumption of ΛCDM. Such values of H_0 are also consistent with the H_0 determination from the tip of the red giant branch (Freedman et al. 2019). However, a smaller tension with SH0ES still remains. There seems to be enough theory space for modifications of the cosmological recombination process that is consistent with these inferred values of $r_{\rm d}$ and H_0 (Di Valentino et al. 2020). Future data will show if it is indeed necessary to amend ΛCDM.

We thank Nikki Arendse and Eiichiro Komatsu for useful discussions. We gratefully acknowledge using `GetDist` (Lewis 2019). This research was enabled in part by support provided by WestGrid (www.westgrid.ca) and Compute Canada Calcul Canada (www.computecanada.ca). L.P. is supported in part by the National Sciences and Engineering Research Council (NSERC) of Canada, and by the Chinese Academy of Sciences President's International Fellowship Initiative, grant No. 2020VMA0020. G.B.Z. is supported by the National Key Basic Research and Development Program of China (No. 2018YFA0404503), a grant of CAS Interdisciplinary Innovation Team, and NSFC grants 11925303, 11720101004, 11673025, and 11890691.

ORCID iDs

Levon Pogosian https://orcid.org/0000-0001-5108-0854
Gong-Bo Zhao https://orcid.org/0000-0003-4726-6714

References

Abazajian, K. N., Adshead, P., Ahmed, Z., et al. 2016, arXiv:1610.02743
Abbott, T. M. C., Abdalla, F. B., Alarcon, A., et al. 2018b, PhRvD, 98, 043526
Abbott, T. M. C., Abdalla, F. B., Annis, J., et al. 2018a, MNRAS, 480, 3879
Addison, G., Watts, D., Bennett, C., et al. 2018, ApJ, 853, 119
Addison, G. E., Hinshaw, G., & Halpern, M. 2013, MNRAS, 436, 1674
Ade, P., Aghanim, N., Arnaud, M., et al. 2016, A&A, 594, A15
Ade, P., Aguirre, J., Ahmed, Z., et al. 2019, JCAP, 02, 056
Aghamousa, A., Aguilar, J., Ahlen, S., et al. 2016, arXiv:1611.00036
Aghanim, N., Akrami, Y., Ashdown, M., et al. 2020a, A&A, 641, A6
Aghanim, N., Akrami, Y., Ashdown, M., et al. 2020b, A&A, 641, A8
Agrawal, P., Cyr-Racine, F.-Y., Pinner, D., & Randall, L. 2019, arXiv:1904.01016
Alam, S., Aubert, M., Avila, S., et al. 2020, arXiv:2007.08991
Anderson, L., Aubourg, É., Bailey, S., et al. 2014, MNRAS, 441, 24
Arendse, N., Wojtak, R. J., Agnello, A., et al. 2020, A&A, 639, A57
Aubourg, E., Bailey, S., Bautista, J. E., et al. 2015, PhRvD, 92, 123516
Aylor, K., Joy, M., Knox, L., et al. 2019, ApJ, 874, 4
Baxter, E. J., & Sherwin, B. D. 2020, arXiv:2007.04007
Beutler, F., Blake, C., Colless, M., et al. 2011, MNRAS, 416, 3017
Bianchini, F., Wu, W. L. K., Ade, P. A. R., et al. 2020, ApJ, 888, 119
Chiang, C.-T., & Slosar, A. 2018, arXiv:1811.03624
Cuceu, A., Farr, J., Lemos, P., & Font-Ribera, A. 2019, JCAP, 10, 044
Cyburt, R. H., Fields, B. D., Olive, K. A., & Yeh, T.-H. 2016, RvMP, 88, 015004
D'Amico, G., Gleyzes, J., Kokron, N., et al. 2020a, JCAP, 05, 005
D'Amico, G., Senatore, L., Zhang, P., & Zheng, H. 2020b, arXiv:2006.12420
Di Valentino, E., Anchordoqui, L. A., Akarsu, O., et al. 2020, arXiv:2008.11284
du Mas des Bourboux, H., Rich, J., Font-Ribera, A., et al. 2020, ApJ, 901, 153
Eisenstein, D. J., Zehavi, I., Hogg, D. W., et al. 2005, ApJ, 633, 560
Freedman, W. L., Madore, B. F., Hatt, D., et al. 2019, ApJ, 82, 34
Gonzalez, M., Hertzberg, M. P., & Rompineve, F. 2020, arXiv:2006.13959
Hart, L., & Chluba, J. 2020, MNRAS, 493, 3255
Hill, J. C., McDonough, E., Toomey, M. W., & Alexander, S. 2020, PhRvD, 102, 043507
Hou, J., Sánchez, A. G., Ross, A. J., et al. 2020, MNRAS, in press
Ivanov, M. M., McDonough, E., Hill, J. C., et al. 2020a, arXiv:2006.11235
Ivanov, M. M., Simonović, M., & Zaldarriaga, M. 2020b, JCAP, 05, 042
Jedamzik, K., & Pogosian, L. 2020, arXiv:2004.09487
Kreisch, C. D., Cyr-Racine, F.-Y., & Dore, O. 2019, arXiv:1902.00534
Lewis, A. 2019, arXiv:1910.13970
Lewis, A., & Bridle, S. 2002, PhRvD, 66, 103511
Lin, M.-X., Benevento, G., Hu, W., & Raveri, M. 2019, arXiv:1905.12618
Magana, J., Amante, M. H., Garcia-Aspeitia, M. A., & Motta, V. 2018, MNRAS, 476, 1036
Mirmelstein, M., Carron, J., & Lewis, A. 2019, PhRvD, 100, 123509
Moresco, M., Pozzetti, L., Cimatti, A., et al. 2016, JCAP, 2016, 014
Murgia, R., Abellán, G. F., & Poulin, V. 2020, arXiv:2009.10733
Pandey, K. L., Karwal, T., & Das, S. 2020, JCAP, 07, 026
Percival, W. J., Sutherland, W., Peacock, J. A., et al. 2002, MNRAS, 337, 1068
Philcox, O. H., Ivanov, M. M., Simonović, M., & Zaldarriaga, M. 2020a, JCAP, 05, 032
Philcox, O. H., Sherwin, B. D., Farren, G. S., & Baxter, E. J. 2020b, arXiv:2008.08084
Poulin, V., Smith, T. L., Karwal, T., & Kamionkowski, M. 2019, PhRvL, 122, 221301
Ratsimbazafy, A., Loubser, S., Crawford, S., et al. 2017, MNRAS, 467, 3239
Reid, M., Pesce, D., & Riess, A. 2019, ApJL, 886, L27
Ross, A. J., Samushia, L., Howlett, C., et al. 2015, MNRAS, 449, 835
Sakstein, J., & Trodden, M. 2019, arXiv:1911.11760
Scolnic, D., Jones, D. O., Rest, A., et al. 2018, ApJ, 859, 101
Sekiguchi, T., & Takahashi, T. 2020, arXiv:2007.03381
Smith, T. L., Poulin, V., Bernal, J. L., et al. 2020, arXiv:2009.10740
Wang, Y., Xu, L., & Zhao, G.-B. 2017, ApJ, 849, 84
Wang, Y., Zhao, G.-B., Zhao, C., et al. 2020, MNRAS, 498, 3470
Wojtak, R. a., & Agnello, A. 2019, MNRAS, 486, 5046
Wu, W., Mocanu, L. M., Ade, P. A. R., et al. 2019, ApJ, 884, 70
Ye, G., & Piao, Y.-S. 2020, arXiv:2008.10832
Zhang, X., & Huang, Q.-G. 2020, arXiv:2006.16692
Zhao, G.-B., Wang, Y., Taruya, A., et al. 2020, arXiv:2007.09011